Heliyon 10 (2024) e41037

Contents lists available at ScienceDirect

Heliyon

journal homepage: www.cell.com/heliyon

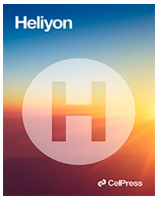

Research article

Intracranial hemorrhage and additional anomalies detected on prenatal magnetic resonance imaging: A large, retrospective study in two tertiary medical institutions

Hao Zhu [a,1], Tianping Wang [b,1], Yuanyuan Lu [c,1], Xiaowei Huang [d], Yu Bai [e], Guofu Zhang [b,**], He Zhang [b,***], Xuan Yin [b,*]

[a] Department of Obstetrics, Obstetrics and Gynecology Hospital, Fudan University, PR China
[b] Department of Radiology, Obstetrics and Gynecology Hospital, Fudan University, PR China
[c] Department of Radiology, Shanghai First Maternity and Infant Health Hospital, School of Medicine, Tongji University, PR China
[d] Department of Ultrasound, Obstetrics and Gynecology Hospital, Fudan University, PR China
[e] Center for Child and Family Policy, Sanford School of Public Policy, Duke University, United States

ARTICLE INFO

Keywords:
Fetus
Magnetic resonance imaging
Intracranial hemorrhages
Fetal malformation

ABSTRACT

Objectives: To clarify the prenatal magnetic resonance (MR) imaging characteristics of fetal intracranial haemorrhages (ICHs) in a large cohort and correlate them with birth outcomes.
Methods: We retrospectively reviewed MR images of fetuses with ICH on screening ultrasound (US) on picture archiving communication system (PACS) servers within a nearly ten-year period from two medical tertiary centres. The indications, main abnormal findings and coexistent anomalies were recorded by two experienced radiologists with census readings.
Results: We recruited 126 cases (average gestational week, 28.0 ± 5.0 weeks) with prenatal MR imaging, including 116 singleton pregnancies and 10 monochromic twin pregnancies. Predominant coexistent anomalies were ventriculomegaly (35.7 %), holoprosencephaly or porencephaly (13.4 %) and enlarged posterior fossa/or posterior fossa cyst (8.7 %) in the lesion-based evaluation. The number of haemorrhagic lesions and the occurrence of the detected complications did not show a correlation with the size of the haematoma. The mass effect of ICH was more commonly observed in the fetus with large for gestational age (GA) than that with small for GA.
Conclusions: Prenatal MR imaging could better show ICH morphology and associated abnormal findings. As a complementary tool of US, MR imaging could help with prenatal counselling and treatment selection after birth.

* Corresponding author. Department of Radiology, Obstetrics and Gynecology Hospital, Fudan University, Shanghai, PR China.
** Corresponding author. Department of Radiology, Obstetrics and Gynecology Hospital, Fudan University, Shanghai, PR China.
*** Corresponding author. Department of Radiology, Obstetrics and Gynecology Hospital, Fudan University, Shanghai, PR China.
E-mail addresses: irios@126.co (H. Zhu), wohong425@163.com (T. Wang), luyuanyuan@51mch.com (Y. Lu), huangxiaowei1476@fckyy.org.cn (X. Huang), yb17@duke.edu (Y. Bai), guofuzh@fudan.edu.cn (G. Zhang), zhanghe1790@fckyy.org.cn (H. Zhang), yinxuan6896@fckyy.org.cn (X. Yin).
[1] These authors contributed equally: Hao Zhu, Tianping Wang and Yuanyuan Lu.

https://doi.org/10.1016/j.heliyon.2024.e41037
Received 28 July 2024; Received in revised form 30 November 2024; Accepted 5 December 2024
Available online 6 December 2024

Abbreviations

ICH	Intracranial hemorrhage
GM-IVH	Germinal matrix intraventricular hemorrhage
MRI	Magnetic resonance imaging
HASTE	Half-Fourier single-shot turbo spin echo
DWI	Diffusion-weighted imaging
US	Ultrasound
VM	Ventriculomegaly
GA	Gestational age
GW	Gestational week
TOP	Termination of pregnancy
FIESTA	Fast imaging employing steady-state acquisition
sIUGR	Selective in-utero growth restriction
TAPs	Twin anemia-polycythemia sequence
TTTS	Twin-twin transfusion syndrome
T1WI	T1-weighted imaging
T2WI	T2-weighted imaging
IVF	In vitro fertilization

Advances in knowledge

- Ventriculomegaly, porencephaly and enlarged posterior fossa were the most prevalent coexistent anomalies in fetuses with ICH.
- The numbers of haemorrhagic lesions and the co-occurrence of detected complications showed no correlation with the volume of haematoma.
- Mass effect associated with ICH was commonly observed in the large-gestational-age fetus.

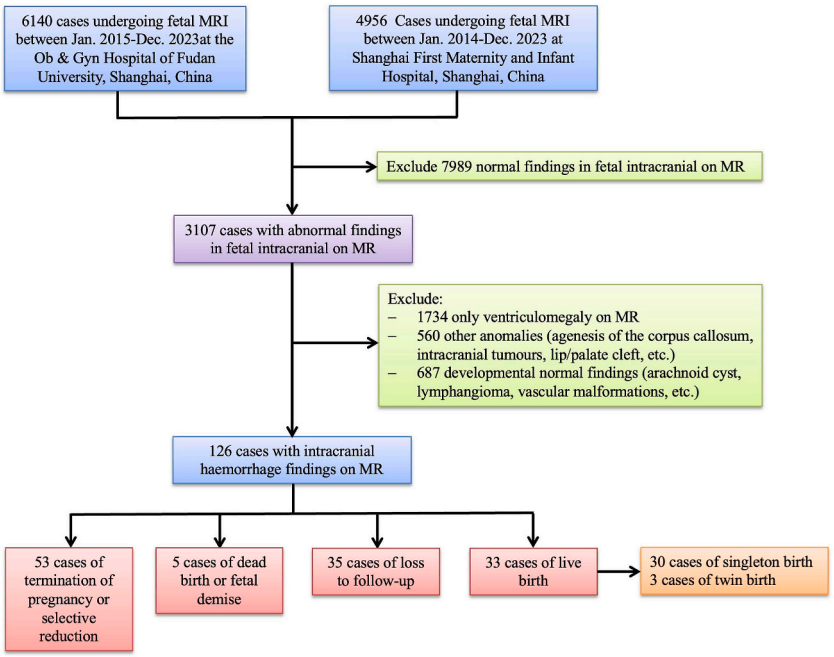

Fig. 1. The flowchart that illustrates the process of patient inclusion in the study.

1. Introduction

Intracranial hemorrhage (ICH) in the fetus is a rare condition with a prevalence of 1/100,000 to 1/1000 in the reported literature [1]. The exact aetiology of fetal brain hemorrhage is unknown. A pregnant woman will not experience any symptoms during an intracranial bleeding process in the fetal head. Previous studies showed it was difficult to detect ICH as early as possible, meaning that the prognoses of these fetuses may be dismal [2,3]. However, with the enhancement of prenatal diagnostic technologies and the improvement of obstetric clinical practices, there is a considerable benefit for pregnant women and perinatal infants. Ultrasonography (US) is the first-choice modality to screen out these suspected abnormal findings [4]. Some subtle lesions are occasionally missed due to either shielding by the calvaria or an uncooperative fetal head position [5]. As a reliable complimentary tool to US, magnetic resonance imaging (MRI) can depict intracranial anatomic structures well and show multiple system anomalies in one scanning plane [6–8]. Unlike MRI characteristics detected in infants or adults, imaging characteristics of fetal ICH vary depending on when and where the haemorrhagic components occur [9]. Coexistent malformations also complicate an accurate diagnosis and evaluation of these abnormal findings on prenatal MRI [10]. To date, reports in the literature on fetal ICH are alarmingly limited, especially in a relatively large cohort study [11,12]. Knowledge of the MRI signs and abnormal findings will help clinicians perform prenatal counselling and treatment selection at term.

Therefore, our purpose in this research is threefold: (1) to describe the primary and secondary MRI characteristics of fetal ICH on prenatal MRI in a large cohort sample from two independent tertiary centres; (2) to summarize the clinical indications and complications for all fetuses with ICH and analyse whether the volume of a haematoma affects the occurrence of coexistent complications detected on MRI; and (3) to correlate these MRI findings with the postnatal outcomes of the fetuses and some follow-up infants.

2. Methods

2.1. Study population

The flow chart of the selected samples was as follows (Fig. 1): first, we retrieved fetal head MR scans from picture archiving communication systems (PACS) in our institution from Jan. 2015 to Dec. 2023 and from another institution from Jan. 2014 to Dec. 2023. All the fetuses underwent MR examination for suspected abnormal central nervous system findings on US or MR performed in a referring hospital. The exclusion criteria included normal findings and only ventriculomegaly reports on MR. Other anomalies (agenesis of the corpus callosum, intracranial tumours, lip/palate cleft, etc.) or developmental abnormal findings (arachnoid cyst, lymphangioma, vascular malformations, etc.) detected on MR were also excluded. Finally, 126 pregnancies were included in this retrospective study (70 pregnancies in our institution and 56 pregnancies in another institution). The gestational age (GA) of all fetuses was verified by the date of the last menstrual period and the US findings in the early trimester. Among them, 10 were twin pregnancies, and the others were singleton pregnancies (Table 1). All women with ongoing pregnancies received multidisciplinary consultations to rule out chromosomal abnormalities through non-invasive prenatal testing or amniocentesis and to exclude intrauterine infection via TORCH laboratory detction. Ethical approval was given by the medical ethics committee of Obstetrics and Gynecology Hospital of

Table 1
Imaging, demographic, and perinatal characteristics of fetal ICH (N = 126).

Parameters	Findings
Maternal age in year (mean ± SD, range)	29.3 ± 4.7 (21–40)
GA in week (mean ± SD, range)	28.0 ± 5.0 (21–40)
Sex (male/female, n %)	60 (47.7 %)/66 (52.3 %)
Mass effect (present/absent, n %)	20(15.8 %)/106(84.1 %)
Multiple/single lesions, n (%)	44/82,65 %
Bigeminal/singleton pregnancy, n (%)	10(7.9 %)/116(92.1 %)
Clinical indications (n %)	
Intracranial hemorrhage	23 (18.3 %)
Ventriculomegaly	25(19.8 %)
Hydrocephalus	12 (9.5 %)
Cerebellum/posterior fossa malformation	8 (6.3 %)
Others (agenesis of corpus callosum, low spinal cord, tethered cord syndrome, TTTs, TAPs, etc.)	58 (46.0 %)
Multiple complications (n %)	
Ventriculomegaly	45 (35.7 %)
Porencephaly or holoprosencephaly	17 (13.4 %)
Enlarged posterior fossa/or posterior fossa cyst	11 (8.7 %)
Agenesis of corpus callosum	3 (2.4 %)
Cerebellar dysplasia/hypoplasia	3 (2.4 %)
Hydrocephalus	14 (11.1 %)
Others (gyri malformation, hydrops fetalis, subependymal cyst, low spinal cord, hydrops fetalis)	17 (13.4 %)
Outcomes	
Termination of pregnancy or selective reduction	53(42.0 %)
Dead birth or fetal demise	5 (4.0 %)
Live birth	33 (26.2 %)
Loss to follow-up	35 (27.8 %)

Fudan University (2020-138).

2.2. MRI acquisition and interpretation

In our hospital, MR was performed using a 1.5-T MR system (Magnetom Avanto, Siemens) with a phased-array coil. All MRI examinations were performed without sedation. The routine MRI protocols used for the assessment of the fetus included axial/sagittal/coronal T2-weighted imaging (T2WI) with half-Fourier acquisition single-shot turbo spin (HASTE) and axial/sagittal/coronal true fast imaging with steady-state precession (True-FISP) sequences and T1-weighted imaging (T1WI) with turbo flash technique. The acquisition parameters for the HASTE sequence were as follows: repetition time (TR) = 1350 ms, echo time (TE) = 92 ms, field of view (FOV) = 400 mm, voxel size: 1.4 × 1.1 × 4.0 mm, flip angle = 170°, matrix = 384 × 256, slice thickness = 4 mm, gap = 0.8 mm, and acquisition time = 20–25s; For the True-FISP sequence were as follows: TR = 3.87 ms, TE = 1.68 ms, FOV = 400 mm, voxel size: 1.7 × 1.6 × 4.0 mm, flip angle = 60°, matrix = 256 × 144, slice thickness = 4 mm, gap = 0.4 mm, and acquisition time = 10–20 s. Diffusion-weighted imaging (DWI) was performed in the axial plane using a two-dimensional echo-planar imaging sequence and parallel acquisition technique, with b values of 0, 100, and 500 s/mm^2. For all MRI sequences, the specific absorption ratio value was controlled under 2.0 W/kg; For T1WI, TR = 2000 ms, TE = 2.45 ms, slice thickness = 4.5 mm.

In another hospital, MR was performed using a 1.5-T MR system (Optima MR 360, GE) with an 8-channel phased-array cardiac coil using the breath-hold technique. The detailed parameters were as follows: fast imaging applying a steady-state acquisition (FIESTA) sequence, TR = 4.4 ms, TE = minimum, FOV = 380 × 380 mm, matrix = 224 × 224, slice thickness/interslice gap = 6/0 mm, bandwidth = 83.13 Hz/pixel; sagittal fast spin-echo (FSE) T2WI, TE = 61 ms; TR = 3000 ms; thickness = 7 mm; gap = 5 mm; FOV = 36 cm; matrix = 320 × 224; number of excitations (NEX) = 2; band = 41. 7 Hz/pixel. Axial T1WI, TE = 11 ms; TR = 830 ms; thickness = 7 mm; gap = 5 mm; FOV = 36 cm; matrix = 320 × 192; NEX = 2; band = 41. 7 Hz/pixel. DWI sequence, TE = 78 ms; TR = 4100 ms; thickness = 8 mm; gap = 6 mm; FOV = 36 cm; matrix = 96 × 128; NEX = 6.

All fetal MRI scans were evaluated independently by two experienced radiologists (both with more than 10 years of experience in fetal MR knowledge) on a PACS terminal server. A four-grade scale was used to evaluate the quality of the images, and it was as follows: Images were classified as excellent (grade 4), which meant having excellent diagnostic image quality without fetal motion artefacts; good (grade 3), indicating moderate artefacts yet with sufficient diagnostic quality; poor (grade 2), referring to having moderate motion artefacts that had an impact on the evaluation of the brain; and unacceptable (grade 1), which signified motion artefacts that seriously affected the image quality as well as the ability to make a diagnosis. On T1WI, the hypointensity, isointensity, and hyperintensity of the amniotic fluid were similar to those of the pelvic wall muscle and subcutaneous fat signal. On T2WI, the hypointensity, isointensity, and hyperintensity of the pelvic bone were similar to those of the pelvic wall muscle and amniotic fluid signal. On b = 800 mm−2/s DWI images, the low and intermediate-signal intensities of the amniotic fluid were similar to those of the cerebral parenchyma.The MRI images were assessed, including (1) the presence of ICH, (2) the location of ICH and the area of the lesion, and (3) the grade of the IVH. The location of the non-GM-IVH (germinal matrix intraventricular hemorrhage) was defined as a haematoma or its debris occurring in the cerebellum, subdural space or corpus callosum. GM-IVH was graded according to the modified Papile classification [13]. The volume of intracranial haematoma was measured by one radiologist based on the reported methods in a previous study [14]. Other coexistent malformations, including ventriculomegaly, holoprosencephaly, hydrocephalus, cerebellar malformations, porencephaly, dilated posterior fossa, agenesis of corpus callosum, etc. were also recorded case-by-case (Table 1).

2.3. Follow-up and delivery outcomes

One obstetrician in this study conducted follow-up during pregnancy and recorded delivery outcomes of each case, including termination of pregnancy (TOP) or selective reduction, dead birth or fetal demise, live birth, and loss to follow-up. The gestational of delivery, delivery mode, birth weight, gender, and Apgar scores of live births were also recorded.

2.4. Statistical analysis

Continuous variables are reported as the median ± standard deviation and range and were compared with Student's t-test. Categorical variables are reported as percentages and were compared with the chi-square test and Fisher's exact test. All analyses were performed using SPSS (version 23.0, IBM). A value of $P < 0.05$ was considered statistically significant.

3. Results

3.1. General information

A total of 126 pregnant women with 116 singletons (average GA: 28.5 ± 5.0, 21–40) and 10 monochromic twin pregnancies (average GA: 24.3 ± 2.5, 21–30) were recruited in this study and underwent prenatal MR imaging. The mean GA for all included pregnancies was 28.0 ± 5.0 (21–40) GWs. Fetus sex differences were not seen in this selected sample (60 males versus 66 females). The main clinical indications for further MR evaluation included intracranial hemorrhage (18.3 %), ventriculomegaly (19.8 %) and hydrocephalus (9.5 %) (Table 1).

3.2. MRI findings

On MR imaging, most ICH in fetuses appeared as a relatively high signal on T1WI (96/126, 76.2 %), an intermediate signal on T2WI (71/126, 56.3 %) and a high signal on DWI (102/126, 80.9 %) in the fetus-based evaluation. The frequency of fetal ICH and their average sizes across gestation are shown in Fig. 2. In this study, GM-IVH (Fig. 3A–E) was seen in 112 pregnancies (average GA: 28.0 ± 4.9 weeks), cerebellar haematoma in 9 pregnancies (average GA: 24.6 ± 1.14 weeks) and haematoma of the corpus callosum (average GA: 36.0 ± 1.0 weeks) in 5 pregnancies. The average volumes of the haematoma for the GM-IVH, cerebellum and corpus callosum were 3.62 ± 7.9, 0.30 ± 0.21 and 0.44 ± 0.26 mm^3, respectively (Table 2). The volume of haemorrhagic components across the various anatomic sites did not differ at the statistical level ($p = 0.705$. There were 73 fetuses with ICH (average size: 1.43 ± 3.35 cm^3) less than 28 GWs and 53 fetuses with ICH (average size: 6.10 ± 10.83 cm^3) more than 28 GWs. The numbers of hemorrhagic lesions and the occurrence of detected complications did not show any dependence on the size of the haematoma (Table 3). However, for fetuses with large GA, the mass effect of the haematoma could be more easily observed due to its relatively large volume ($p = 0.002$). Thirty-seven fetuses with ICH had one coexistent malformation or abnormal finding, 20 had multiple complications and 23 had no complications on MR imaging. Ventriculomegaly (35.8 %, Fig. 4A–C), holoprosencephaly or porencephaly (13.6 %, Fig. 4A–C) and enlarged posterior fossa/or posterior fossa cysts (7 %) were the three most commonly detected abnormal findings in the lesion-based evaluation. Brain infarction (Fig. 3A–E) and oedema (Fig. 5A–D) were also encountered as rare complications related to fetal ICH in this study group.

3.3. Follow-up and delivery outcomes

A total of 35 cases loss to follow-up. Overall, 53 TOP, 1 dead birth and 4 fetal demise, and 33 livebirths were recorded in the present study. Of 33 livebirth pregnant women, there were 30 singleton pregnancies and 3 twin pregnancies. The delivery outcomes of their 34 livebirths were showed in Supplementary Table 1. The average GA at delivery of singleton livebirths was 37.6 ± 2.2 weeks, and the outcomes were promising. One live infant with ICH detected on prenatal MR imaging from a singleton pregnancy had definite neurological symptoms (Fig. 6A–C). His chromosomal microarray analysis results revealed a de novo mutation of PLOD1, which is associated with Ehlers–Danlos syndrome. One case of hydrops fetalis with alloimmune haemolysis was also detected. The volume of haemorrhagic components did not show a correlation with the final outcomes in the present study. Supplementary Table 2 showed the indications, MR findings and outcomes of the 3 livebirth twin pregnancies. One pregnant woman with a twin anaemia-polycythemia sequence (Taps) delivered both healthy infants (Fig. 7A–F). One pregnancy with twin-twin transfusion syndrome (TTTs) stage 4, reduction surgery performed for one fetus and expectation treatment for another with hydrops fetalis was applied and delivered at 28^{+2} weeks' GA. In one TTT stage 1 twin pregnancy, one fetus was in utero dead, and another fetus was a live birth with premature delivery (Fig. 8A–F).

4. Discussion

We conducted a retrospective study reviewing MRI characteristics in fetuses with ICH and their co-occurrence abnormal findings in a large cohort ten-year sample from two tertiary centres. We found that fetal ICH could occur at any time across gestation and had various appearances depending on the onset time as observed on MR imaging. GM-IVH was the most common site of the intracranial bleeding. Ventriculomegaly (45 cases) was the most common coexistent abnormal finding on MRI, followed by porencephaly or holoprosencephaly (17 cases) and enlarged posterior fossa/or posterior fossa cysts (11 cases) in the present studied samples. We did not find a correlation between the haematoma volume and the final outcomes.

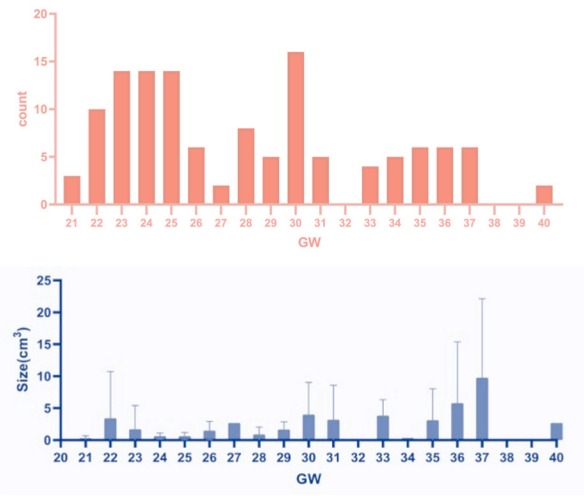

Fig. 2. The frequency of fetal ICH and their average sizes across gestation in the present included samples.

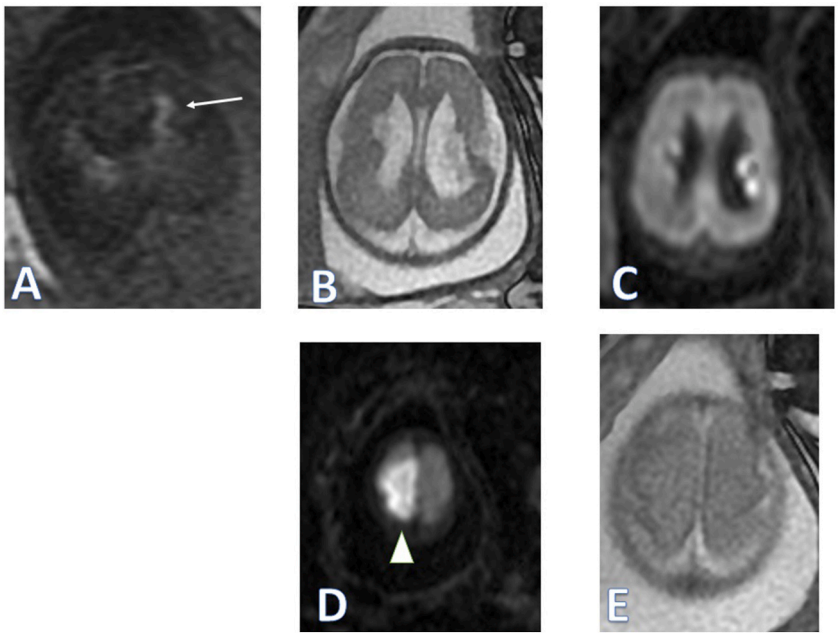

Fig. 3. A 28-GW singleton pregnancy. The GM-IVH components (arrow) were detected on T1WI (A), T2WI (B) and DWI (C). On the upper plane, a patchy high signal (arrowhead) indicating early cerebral infarction in the frontal-parietal lobe was also displayed on DWI (D), which did not show any abnormal signal on the corresponding T2WI (E).

Table 2
MR imaging characteristics of fetal intracranial parenchyma hemorrhage across various anatomic sites on fetus-based evaluation.

	GM-IVH	Corpus callosum	Cerebellum	P value
Total	112	5	9	
Average GA	28.0 ± 4.9	36.0 ± 1.0	24.6 ± 1.14	0.007
Average Size(cm^3)*	3.62 ± 7.9	0.44 ± 0.26	0.30 ± 0.21	0.705
Grade	2.59 ± 1.1	–	–	
Observed Mass effect	19	–	1#	0.549
Coexistent malformation (Num. %)	98 (77.8 %)	–	–	<0.001

GM-IVH, germinal matrix intraventricular hemorrhage; * the lesion could not be outlined in six cases; #this case also had GM-IVH.

Table 3
The detected complications associated with intracranial hemorrhage in fetuses on MR Imaging by various size and gestational weeks' group.

	≤28 GW		>28 GW		Total
	Average hemorrhagic area size (1.43 ± 3.35 cm^3)		Average hemorrhagic area size (6.10 ± 10.83 cm^3)		
	≤5	>5	≤5	>5	
Complications (Num.)(n = 126)					
Single	39	1	29	7	
Multiple	30	3	11	6	
p value					0.157
Mass effect (Num.)(n = 126)					
Observed	4	3	6	7	
Non-observed	60	6	30	10	
p value					0.002
Outcomes (Num.) (n = 91)					
Live	15	0	16	2	
TOP/fetus reduction	31	3	16	3	
Dead birth/fetal demise	1	1	1	2	
p value					0.174

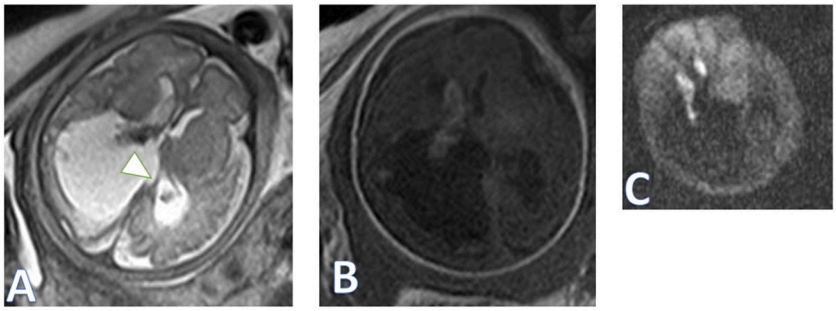

Fig. 4. A 25-GW singleton pregnancy. The GM-IVH mainly seen on one side of the lateral ventricle with both obvious enlargement of the ipsilateral posterior horn of the lateral ventricle and thinness of the adjacent grey matter in the occipital lobe on T1WI (A), T2WI (B) and DWI (C). The porencephaly was also seen in the occipital lobe (arrowhead). The TOP procedure was performed.

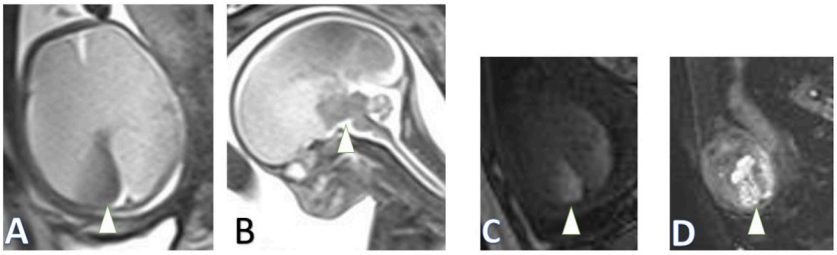

Fig. 5. A 22-GW singleton pregnancy. A diffuse iso-hyperintensity signal was seen in both cerebral hemispheres with diffuse loss of grey–white differentiation and effacement of the sulci on HASTE (A–B). The occipital lobe, thalamus and brainstem (arrowhead) mostly displayed iso-hypointensity signals on T2WI (B), slightly high signals on T1WI (C) and extremely restricted signals on DWI (D). All of these signs indicated postbleeding changes with diffuse cerebral oedema in the brain parenchyma. The TOP procedure was performed.

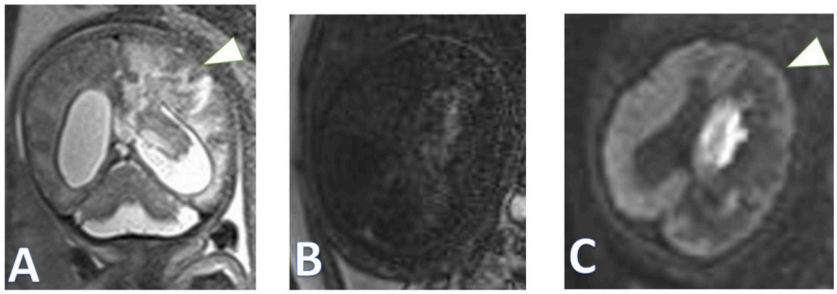

Fig. 6. A 37-GW singleton pregnancy. A giant GM-IVH haematoma had shifted the midline a little on T2WI (A) and T1WI (A). The volume of the involved cerebral parenchyma decreased more than on the normal side (arrowhead). This character can be seen more clearly on DWI images (C). This case also had TCS syndrome (not shown). After birth, a V-P shunting procedure at 2 months old was performed. The main symptoms included muscle weakness with normal defecation function.

It has been reported that ICH is more often detected in premature infants than in prenatal life [1]. However, even if detected, the prognoses for these fetuses are dismal. Fetal ICH can be identified with both in utero US and MR imaging. The advantages of MR include better soft tissue resolution and simultaneous evaluation of multisystem malformations in one scan [15]. On fetal MR, the characteristics of ICH show an atypical signal because ICH is occasionally detected or suspected on routine US screening of pregnancies. At this time, fetuses will exhibit no specific symptoms. In this study, most ICHs were magnified as relatively high signals on T1WI, intermediate signals on T2WI and high signals on DWI. The margin of the haematoma could be better outlined on DWI (Figs. 4–6) than in the other two protocols. Furthermore, we also calculated the size of the haemorrhagic components in each case (similar results were not reported in the previously published literature) and found that the volume of the detected haematoma seemed larger in the late gestation than in the early gestation. However, the volume of the haematoma did not show a significant difference across either the gestation or the anatomic compartments at the statistical level. In one study, the authors reported that GM-IVH occurred more frequently and later in pregnancy than non-GM hemorrhage [16]. In our study, both GM-IVH and cerebellum [17] bleeding occurred in early pregnancy, and corpus callosum hemorrhage was only detected in later pregnancy. However, due to the

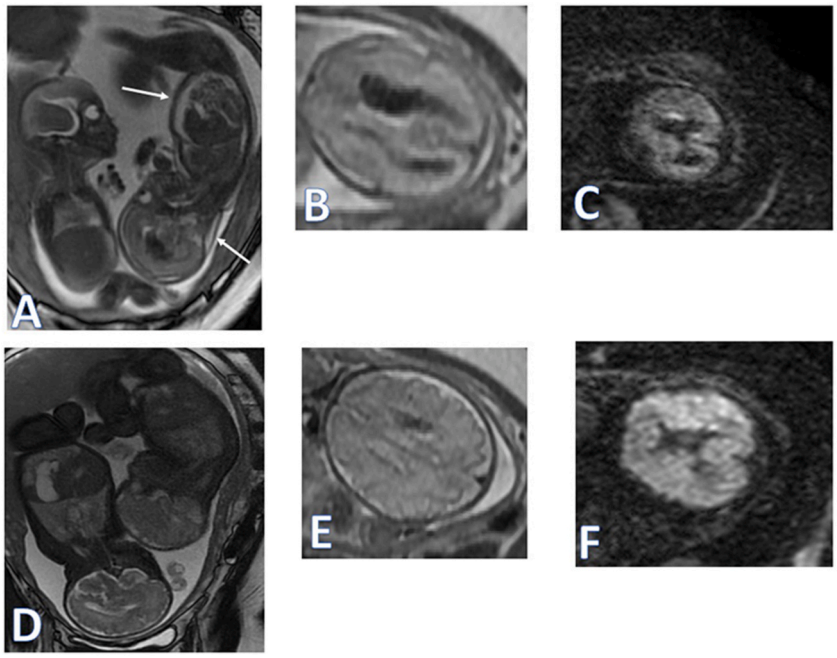

Fig. 7. A 25-GW monochorionic twin pregnancy. One fetus had haemorrhagic components in the lateral ventricle on FIESTA images (A). GM-IVH displayed an extremely low signal on both T2WI (B) and DWI (C). Note that the ascites and hydrops fetalis are shown (arrow). On seven-week follow-up MR (D–F), this fetus grew as well as the normal fetus according to the estimated growth trend (D), and both the ascites and hemorrhage components largely resolved (E–F). The patient had a caesarean delivery at 35 GW (birth weight: 2220 g/1890 g, 1-min Apgar score: 9/9).

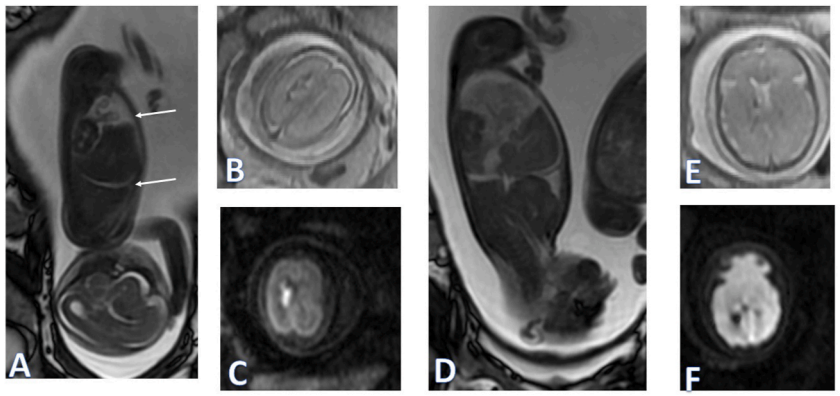

Fig. 8. A 25-GW TTTS stage 1 fetus in monochorionic twin pregnancy. One fetus had bleeding components (A) in the lateral ventricle on FIESTA images. Note that pleural effusion and ascites are shown (arrow). The band of the low signal in the adjacent parenchyma was also detected on the SS FSE image (B) and DWI (C). On three-week follow-up MR (D–F), both pleural effusion and ascites continued to grow (D). The hemorrhage components in the ventricle seemed to be resolved to some extent (E/F). However, subsequent US did not detect a fetal heartbeat and confirmed intrauterine fetal death. The other fetus (not shown) was delivered at 31 GW (birth weight: 1205 g, 1 min Apgar score: 9).

limited number of included samples, this needs to be validated in a larger sample.

Many causes could be responsible for fetal ICH, including infectious disease, maternal drug exposure, alloimmune thrombocytopenia, maternal trauma, coagulation disorders, twin-to-twin transfusion syndrome (TTTs), etc. [18]. A genetic disorder should be taken into account as the potential cause for many indeterminate cases. In the present study, we only performed gene analysis in one case (Fig. 6). For all 10 twin pregnancies in the included samples, TTTs was the most common indication (6/10) for fetal ICH evaluation [19]. In terms of coexistent complications, 65 (51.6 %) cases had abnormal findings apart from ventriculomegaly on in utero MR. For singleton pregnancies, 3 fetuses with ICH had gyri malformations, 1 fetus had TCS, and 13 fetuses with porencephaly were observed in this study. For twin pregnancies, hydrops fetalis was the most commonly detected abnormal finding, although this complication may not be associated with fetal ICH itself. Furthermore, in this study, the number of haemorrhagic lesions did not show a correlation with the haematoma volume but had some correlations with the haematoma mass effect itself. In the present study, 58

pregnancies had the final outcome recorded by either correspondence with the involved patients or by searching the inpatient medical records through a hospital information system. Among them, 1 dead birth and 2 fetal deaths (one in a singleton and one in a twin pregnancy) were recorded. Additionally, the volume of haemorrhagic components did not show a correlation with the final outcomes in the present study [17]. Neurodevelopmental outcomes were not evaluated owing to the short follow-up period. Comparatively, twin pregnancies have more complicated complications and poor prognoses [20]. On the one hand, these pregnancies had predisposed disease (herein, TTTs are the underlying aetiology); on the other hand, some invasive reduction surgery was performed for fetuses with growth restriction. A large amount of haematoma was not observed in this cohort of twin pregnancies on prenatal MR.

Our study has some limitations. First, a relatively small number of infants were followed up after birth. A longer follow-up time will help better assess the neurodevelopmental outcome for fetuses with ICH in utero. A high rate of termination of pregnancy can underestimate the occurrence of adverse outcomes. Second, in this study, 1.5T MR equipment was applied. Although it has not yet been well evaluated for intrauterine examinations, 3.0T fetal MR with a high signal-to-noise ratio and fast scanning protocols may improve the image resolution [21]. Future studies will help to clarify the differences in imaging characteristics in fetal ICH between these two MR strengths. These findings will assist clinical decision making, providing better prenatal assessments and benefits for perinatal infants.

5. Conclusion

Prenatal MR imaging could better show the ICH morphology and the associated abnormal findings. As a complementary tool of US, MR imaging could help with prenatal counselling and treatment selection after birth.

CRediT authorship contribution statement

Hao Zhu: Writing – original draft. **Tianping Wang:** Methodology, Data curation. **Yuanyuan Lu:** Formal analysis. **Xiaowei Huang:** Resources. **Yu Bai:** Methodology, Formal analysis. **Guofu Zhang:** Writing – review & editing. **He Zhang:** Writing – review & editing, Conceptualization. **Xuan Yin:** Writing – review & editing.

Availability of data and materials

The authors confirm that the data supporting the findings of this study are available within the article.

Data and code availability statement

Data included in article/supplementary material is referenced in the article.

Declaration of competing interest

The authors declare that they have no known competing financial interests or personal relationships that could have appeared to influence the work reported in this paper.

Appendix A. Supplementary data

Supplementary data to this article can be found online at https://doi.org/10.1016/j.heliyon.2024.e41037.

References

[1] A.F. Cavaliere, I. Turrini, M. Pallottini, A. Vidiri, L. Marchi, F. Perelli, et al., Genetic profiling of idiopathic antenatal intracranial haemorrhage: what we know? Genes 12 (4) (2021) 573, https://doi.org/10.3390/genes12040573.
[2] Özköse Z. Gedik, S.C. Oğlak, A. Bestel, M. Behram, S. Süzen Çaypınar, F. Ölmez, et al., Fetal intracranial hemorrhage: prenatal sonographic diagnosis criteria and postnatal outcomes, J. Turk. Ger. Gynecol. Assoc. 23 (4) (2022) 268–274, https://doi.org/10.4274/jtgga.galenos.2021.2021-0042.
[3] F.G. Sileo, J. Zöllner, F. D'Antonio, S. Islam, A.T. Papageorghiou, A. Khalil, Perinatal and long-term outcome of fetal intracranial hemorrhage: systematic review and meta-analysis, Ultrasound Obstet. Gynecol. 59 (5) (2022) 585–595, https://doi.org/10.1002/uog.24766.
[4] B.J. van der Knoop, I.A. Zonnenberg, J.I.M.L. Verbeke, L.S. de Vries, L.R. Pistorius, M.M. van Weissenbruch, et al., Additional value of advanced neurosonography and magnetic resonance imaging in fetuses at risk for brain damage, Ultrasound Obstet. Gynecol. 56 (3) (2020) 348–358, https://doi.org/10.1002/uog.21943.
[5] J.N. Karim, N.W. Roberts, L.J. Salomon, A.T. Papageorghiou, Systematic review of first-trimester ultrasound screening for detection of fetal structural anomalies and factors that affect screening performance, Ultrasound Obstet. Gynecol. 50 (4) (2017) 429–441, https://doi.org/10.1002/uog.17246.
[6] B. Putbrese, A. Kennedy, Findings and differential diagnosis of fetal intracranial haemorrhage and fetal ischaemic brain injury: what is the role of fetal MRI? Br. J. Radiol. 90 (1070) (2017) 20160253 https://doi.org/10.1259/bjr.20160253.
[7] A. Tanacan, B. Ozgen, E. Fadiloglu, C. Unal, K.K. Oguz, M.S. Beksac, Prenatal diagnosis of central nervous system abnormalities: neurosonography versus fetal magnetic resonance imaging, Eur. J. Obstet. Gynecol. Reprod. Biol. 250 (2020) 195–202, https://doi.org/10.1016/j.ejogrb.2020.05.013.
[8] L. Manganaro, S. Bernardo, A. Antonelli, V. Vinci, M. Saldari, C. Catalano, Fetal MRI of the central nervous system: state-of-the-art, Eur. J. Radiol. 93 (2017) 273–283, https://doi.org/10.1016/j.ejrad.2017.06.004.

[9] T. Wang, J. Wang, S. Cai, G. Zhang, T. Sun, Z. Fu, et al., Magnetic resonance imaging evaluation of foetal intracranial haemorrhage and the correlation with ultrasound findings and postnatal outcomes, Arch. Gynecol. Obstet. 305 (4) (2022) 877–884, https://doi.org/10.1007/s00404-021-06210-8.
[10] E. Miller, G. Orman, T.A.G.M. Huisman, Fetal MRI assessment of posterior fossa anomalies: a review, J. Neuroimaging 31 (4) (2021) 620–640, https://doi.org/10.1111/jon.12871.
[11] K.N. Epstein, B.M. Kline-Fath, B. Zhang, C. Venkatesan, M. Habli, D. Dowd, et al., Prenatal evaluation of intracranial hemorrhage on fetal MRI: a retrospective review, AJNR Am J Neuroradiol 42 (12) (2021) 2222–2228, https://doi.org/10.3174/ajnr.A7320.
[12] E.J. Snyder, S. Pruthi, M. Hernanz-Schulman, Characterization of germinal matrix hemorrhage in extremely premature infants: recognition of posterior location and diagnostic pitfalls, Pediatr. Radiol. 52 (1) (2022) 75–84, https://doi.org/10.1007/s00247-021-05189-3.
[13] R. Starr, O. De Jesus, S.D. Shah, J. Borger, Periventricular and intraventricular hemorrhage, in: StatPearls [Internet]. Treasure Island (FL): StatPearls Publishing; Copyright © 2021, StatPearls Publishing LLC., 2024, 2021. Available from: http://www.ncbi.nlm.nih.gov/books/NBK538310/.
[14] B. Zhao, W.B. Jia, L.Y. Zhang, T.Z. Wang, 1/2SH: a simple, accurate, and reliable method of calculating the hematoma volume of spontaneous intracerebral hemorrhage, Stroke 51 (1) (2020) 193–201, https://doi.org/10.1161/STROKEAHA.119.026951.
[15] U.D. Nagaraj, B.M. Kline-Fath, Clinical applications of fetal MRI in the brain, Diagnostics 12 (3) (2022) 764, https://doi.org/10.3390/diagnostics12030764.
[16] L. Sanapo, M.T. Whitehead, D.I. Bulas, H.K. Ahmadzia, L. Pesacreta, T. Chang, et al., Fetal intracranial hemorrhage: role of fetal MRI, Prenat. Diagn. 37 (8) (2017) 827–836, https://doi.org/10.1002/pd.5096.
[17] S.J. Steggerda, F.T. De Bruïne, A.A. van den Berg-Huysmans, M. Rijken, L.M. Leijser, F.J. Walther, et al., Small cerebellar hemorrhage in preterm infants: perinatal and postnatal factors and outcome, Cerebellum 12 (6) (2013) 794–801, https://doi.org/10.1007/s12311-013-0487-6.
[18] M. Hausman-Kedem, G. Malinger, S. Modai, S.A. Kushner, S.I. Shiran, L. Ben-Sira, et al., Monogenic causes of apparently idiopathic perinatal intracranial hemorrhage, Ann. Neurol. 89 (4) (2021) 813–822, https://doi.org/10.1002/ana.26033.
[19] J.S. Moldenhauer, M.P. Johnson, Diagnosis and management of complicated monochorionic twins, Clin. Obstet. Gynecol. 58 (3) (2015) 632–642, https://doi.org/10.1097/GRF.0000000000000127.
[20] D. Di Mascio, A. Khalil, A. D'Amico, D. Buca, P. Benedetti Panici, M.E. Flacco, et al., Outcome of twin-twin transfusion syndrome according to Quintero stage of disease: systematic review and meta-analysis, Ultrasound Obstet. Gynecol. 56 (6) (2020) 811–820, https://doi.org/10.1002/uog.22054.
[21] J. Neelavalli, U. Krishnamurthy, P.K. Jella, S.S. Mody, B.K. Yadav, K. Hendershot, et al., Magnetic resonance angiography of fetal vasculature at 3.0 T, Eur. Radiol. 26 (12) (2016) 4570–4576, https://doi.org/10.1007/s00330-016-4243-4.